TRACING THE ELECTRON DENSITY FROM THE CORONA TO 1 AU

YOLANDE LEBLANC, GEORGE A. DULK and JEAN-LOUIS BOUGERET
Observatoire de Paris, DESPA, URA 264 CNRS, 92195 Meudon, France

(Received 5 March 1998; accepted 2 June 1996)

Abstract. We derive the electron density distribution in the ecliptic plane, from the corona to 1 AU, using observations from 13.8 MHz to a few kHz by the radio experiment WAVES aboard the spacecraft Wind. We concentrate on type III bursts whose trajectories intersect the spacecraft, as determined by the presence of burst-associated Langmuir waves, or by energetic electrons observed by the 3-D Plasma experiment. For these bursts we are able to determine the mode of emission, fundamental or harmonic, the electron density at 1 AU, the distance of emission regions along the spiral, and the time spent by the beams as they proceed from the low corona to 1 AU. For all of the bursts considered, the emission mode at burst onset was the fundamental; by contrast, in deriving many previous models, harmonic emission was assumed.

By measuring the onset time of the burst at each frequency we are able to derive an electron density model all along the trajectory of the burst. Our density model, after normalizing the density at 1 AU to be $n_e(215\ R_0) = 7.2\ \mathrm{cm}^{-3}$ (the average value at the minimum of solar activity when our measurements were made), is $n_e = 3.3 \times 10^5\ r^{-2} + 4.1 \times 10^6\ r^{-4} + 8.0 \times 10^7\ r^{-6}\ \mathrm{cm}^{-3}$, with r in units of R_0. For other densities at 1 AU our result implies that the coefficients in the equation need to be multiplied by $n_e(1\ \mathrm{AU})/7.2$.

We compare this with existing models and those derived from direct, *in-situ* measurements (normalized to the same density at 1 AU) and find that it agrees very well with *in-situ* measurements and poorly with 'radio models' based on apparent source positions or assumptions of the emission mode. One implication of our results is that isolated type III bursts do not usually propagate in dense regions of the corona and solar wind, as it is still sometimes assumed.

1. Introduction

Solar type III bursts are generated by beams of energetic electrons ejected from the Sun that travel outward along open magnetic field lines through the corona and interplanetary space. Along their path they generate Langmuir waves at the plasma frequency f_p, and some of the energy of the Langmuir waves is converted into electromagnetic radiation either at the fundamental, $f = f_p$, the second harmonic, $f = 2f_p$, or both. In situ, electrons and Langmuir waves have been directly associated with type III emission.

The plasma frequency f_p is directly related to the electron density by the relation $f_p \approx 9 \times n_e^{1/2}$, where f_p is in kHz and n_e is the electron number density in cm^{-3}. Therefore, with knowledge of the mode of emission (fundamental $f = f_p$ or harmonic $f = 2f_p$) and observations over a large frequency range from a few MHz to a few kHz, it is possible with few assumptions to trace the electron density from the corona to 1 AU and beyond.

Solar Physics **183:** 165–180, 1998.

First we summarize various means of deriving the density of the corona and solar wind.

1.1. CORONAGRAPH OBSERVATIONS

Close to the Sun, coronal density models have been derived from eclipse observations at visible wavelengths. These provide densities from about 1 to 3 R_0 (Baumbach, 1937; van de Hulst, 1950; Newkirk, 1967; Saito, 1970; Leblanc, Leroy, and Pecantet, 1973; Koutchmy and Livshits, 1992). The white-light coronagraph data of *Skylab* were used to determine the density of the corona from 2.5 to 5.5 R_0 (Saito, Poland, and Munro, 1977). In the near future the LASCO observations should be able to extend the coronal models up to 30 R_0 (Vibert, 1997). By contrast the radio technique used here yields the density along the trajectory of the type III bursts from the middle corona to 1 AU and beyond, but not at very low heights, $r \lesssim 1.2\ R_0$.

In the low corona, $r \lesssim 1.1\ R_0$, the density gradient is very steep; for example, Baumbach (1937) was the first to develop an expression where in this height range $n_e \sim r^{-16}$. Then at $1.1 \lesssim r \lesssim 2.3\ R_0$ he found $n_e \sim r^{-6}$, and at $r \gtrsim 2.3\ R_0$ he found $n_e \sim r^{-1.5}$.

1.2. IN-SITU OBSERVATIONS

In interplanetary space, *in-situ* measurements of electron density were made by Bougeret, King, and Schwenn (1984) from 0.3 to 1 AU. These authors used *in-situ* observations by the *Helios 1* and *2* spacecraft and derived the density model $n_e = 6.1\ R^{-2.1}\ \mathrm{cm}^{-3}$ where R is in AU. This model is the most reliable up to now since it is derived from direct measurements without any assumptions. The authors remark that their model gives densities lower than the 'radio' density models, which is not surprising because most of the latter were constructed using observed positions of sources, i.e., of scattered images that are higher than the true sources.

Recently, Issautier *et al.* (1997) measured the average electron density at about 1.4 AU during the passage of *Ulysses* through the ecliptic plane; extrapolated to 1 AU they find a mean electron density of 7.2 cm^{-3} which is very similar to the value 6.1 of Bougeret, King, and Schwenn. In addition, Issautier *et al.* (1998) found a radial variation of the electron density $n_e \sim r^{-2.003}$ at high latitudes (greater than 40°), between 1.52 and 2.31 AU. Earlier, Davis and Feynman (1977) from a type II burst analysis, suggested a variation $\sim r^{-2}$ for $r > 100\ R_0$.

1.3. REMOTE SENSING OBSERVATIONS

1.3.1. *Frequency Drift Rates of Radio Bursts*

This method has been used by authors who measured the frequency drift rate of type III or type II bursts (Hartz, 1969; Haddock and Alvarez, 1973; Alvarez and Haddock, 1973; Malitson, Fainberg, and Stone, 1973). At the time of these studies

the mode of emission was not known, and it was usually assumed that it was the harmonic. In hindsight, we now believe the bursts analyzed were probably a mixture of fundamentals and harmonics. The assumption of harmonic emission leads to a model that is less dense by a factor of 4 compared to one where emission at the fundamental is assumed. Then the discrepancy is less between the 'radio' models and coronal models derived from K-corona observations. There is no theoretical support to assume an emission at harmonic rather than at fundamental (Melrose, 1982; Robinson, 1996), and there is now evidence for fundamental emission in the cases of bursts associated with electron streams and Langmuir waves observed *in situ* (Kellogg, 1980; Dulk, Steinberg, and Hoang, 1984; Dulk *et al.*, 1987, 1998; Hoang, Dulk, and Leblanc, 1994). When there are no electron streams or Langmuir waves, there is no direct way to distinguish fundamental from harmonic emission, but indirect evidence implies that both modes are present, with the harmonic mode being the more prevalent for bursts whose electron streams are directed well away from the spacecraft.

The drift rates of type III bursts at metric wavelengths have been used to estimate the speed of electron streams creating the bursts, and indirectly the coronal density at $r \lesssim 1.2\ R_0$. The measured drift rates, combined with an estimated coronal scale height $H \approx 10^5$ km, lead to an electron speed of about $0.3\ c$ (Poquerusse, Hoang, and Bougeret, 1996), i.e., two times larger than is implied by observations at decameter and longer wavelengths. Either the electron exciter speed decreases by a factor of two from the low to the middle or upper corona, or the scale height of the low corona is overestimated by a factor of two. Regarding a decrease of electron speeds, there is no independent evidence for any deceleration from the corona to more than 1 AU. Regarding the scale height of the low corona, Baumbach (1937; see Section 1.1) used eclipse observations and derived the relation $n_e \sim r^{-16}$ at $r \lesssim 1.1\ R_0$, for which the scale height is $H \approx 0.45 \times 10^5$ km, about a factor of two smaller than the 10^5 km mentioned above.

1.3.2. *Observed Radial Distances*

Given that radio spectral observations do not give the radial distance of emission directly, sometimes the observed frequency has been related to the radial distance through spatial resolution of the source positions. Unfortunately, when the radial distance is directly observed (Wild, Sheridan, and Neylan, 1959; Fainberg and Stone, 1974; Gurnett, Baumback, and Rosenbauer, 1978; Stone, 1980; Reiner *et al.*, 1998) it is of an *apparent* position of the source, i.e., the scatter image after the radiation has been scattered by inhomogeneities in the corona or solar wind (Steinberg *et al.*, 1971; Leblanc, 1973), and this position is higher than the true source by one to two density scale heights (e.g., higher by $\approx 0.3\ R_0$ at $1.5\ R_0$ (Stewart, 1976) and 0.3 AU at 0.5 AU (Dulk, Steinberg, and Hoang, 1984)). Thus, this scattering is most important at the longer wavelengths. The result is that models based on observed source positions are overdense, and when compared with the density models derived from coronagraph or *in situ* observations, these radio models are

higher by a factor of ten or more (e.g., Wild, Smerd, and Weiss, 1963; Bougeret, King, and Schwenn, 1984, and references therein).

While there are occasional reports of correspondences between radio positions and coronal jets or bright features (Kundu *et al.*, 1983), there is no statistical evidence that type IIIs consistently propagate along dense structures. The statistical studies (Leblanc, Kuiper, and Hansen, 1974; Smerd, private communication; Leblanc and de la Noe, 1977; Poquerusse *et al.*, 1988; Steinberg *et al.*, 1984) show that the sources of type III bursts rarely lie on dense structures in the corona. Instead they propagate along open field lines in the normal corona, that is, occasionally in overdense regions, occasionally in underdense regions, and frequently in average regions.

The purpose of this paper is to derive the electron density distribution from the low corona to 1 AU using observations made by the radio experiment WAVES aboard the spacecraft *Wind*. These observations cover the unprecedentedly large frequency range from 13.8 MHz to a few kHz. In addition the associated Langmuir waves and/or energetic electrons are observed by the spacecraft, and the local plasma frequency at 1 AU is measured from the quasi-thermal plasma line. We concentrate on type III bursts whose trajectories intersect the spacecraft, as determined by the presence of burst-associated Langmuir waves or energetic electrons observed by the 3-D Plasma experiment (Lin *et al.*, 1995). For these bursts we are able to determine the mode of emission F or H, the electron density at 1 AU, the distance of emission regions along the spiral, and the time spent by the beams as they proceed from the low corona to 1 AU. By measuring the starting time of the burst at each frequency we are able to derive an electron density model all along the trajectory of the burst. In Section 2 we briefly describe the observational techniques and present electron and radio data of a sample event. In Section 3, we derive the drift rate and the density model. In Section 4 we compare with other models and conclude.

2. Observations and a Sample Event

The *Wind* spacecraft is always near Earth, in the ecliptic plane, near 1 AU. Radio waves are observed from remote locations, from near the Sun to more than 1 AU, and from bursts that originate anywhere, even directly behind the Sun. Here we concentrate on bursts for which *Wind* was within the path of the electron streams, where the impulsive electron fluxes were observed with the 3-D Plasma and Energetic Particle experiment (Lin *et al.*, 1995); the associated Langmuir waves and solar type III bursts were observed with the WAVES instrument (Bougeret *et al.*, 1995). Combining the data from the two experiments allows the study of the characteristics of events observed simultaneously.

2.1. METHOD OF ANALYSIS

For the electrons that produce the type III burst, we derive their average speed along the Archimedean spiral ($v_{\rm elec}$) by measuring the time interval from burst onset near the corona to the onset of Langmuir waves at 1 AU or of fast electrons estimated to be in an unstable distribution. Burst onset at 1 R_0 ($t_{\rm init}$), is determined from the highest frequency measured (usually 13.8 MHz), extrapolated to 1 R_0. We measure the electron density at 1 AU from the plasma line produced by thermal motions of the electrons in the vicinity of the spacecraft (Meyer-Vernet and Perche, 1989). The discrimination between fundamental and harmonic is evident from the trace of onset times vs frequency and the extrapolation to the onset of Langmuir waves (Dulk, Steinberg, and Hoang, 1984).

Then from $v_{\rm elec}$, $t_{\rm init}$ and the onset times at each of (usually) 32 frequencies, we derive the distance along the Archimedean spiral of the emission at each frequency, and then we calculate the corresponding radial distance. Hence, for each measured frequency f, where $f = f_p = 9\sqrt{n_e}$ for F radiation, we have the electron density and the radial distance.

2.2. THE OBSERVATIONS

For this study we consider 11 type III bursts, 7 of which were used for another study by Dulk *et al.* (1998). These type III bursts occurred in the period of December 1994 to November 1997, near the minimum of solar activity. These bursts were observed from 13.8 MHz to about 20 kHz, and one of them was also observed from 75 to 25 MHz with the decameter array of Nançay (Boischot *et al.*, 1980). They were all associated with Langmuir waves and/or electron events. In each case it was demonstrated that the mode of emission was fundamental.

Figure 1 shows a dynamic spectrum of the burst occurring at 10:40 UT on 27 December 1994. The burst is very intense, well isolated from the following burst at 12:00 UT, and drifts down from 13.8 MHz almost to 20 kHz. The plasma frequency at 1 AU decreases slowly from about 24 to 19 kHz in the three hours leading up to the burst as can be seen from the plasma line at f_p and the $2f_p$ line related to the Earth's bow shock. The sudden intensification of the plasma line at 11:45 UT demonstrates the commencement of Langmuir waves. The Langmuir waves continue for about an hour. Energetic electrons in the 100 to 1 keV range were observed by the 3D Plasma experiment during the event.

Figure 2 shows the times of burst onset at 16 frequencies in the band from 1 MHz to 19 kHz (stars), the times of the peak flux density (triangles), and the interval of occurrence of Langmuir waves at 19 kHz (squares). Knowing that f_p(1 AU) is 19 kHz and that the plasma frequency in the solar wind varies as $f_p \sim r^{-1.05}$ ($n_e \sim R^{-2.10}$; see Section 1 and Bougeret, King, and Schwenn, 1984), we convert the frequency scale of the right-hand ordinate to the radial distance scale of the left-hand ordinate. We then derive the average speed of the exciting electrons $v_{\rm elec} = D/\Delta t$, where D is the path length travelled along an Archimedean spiral,

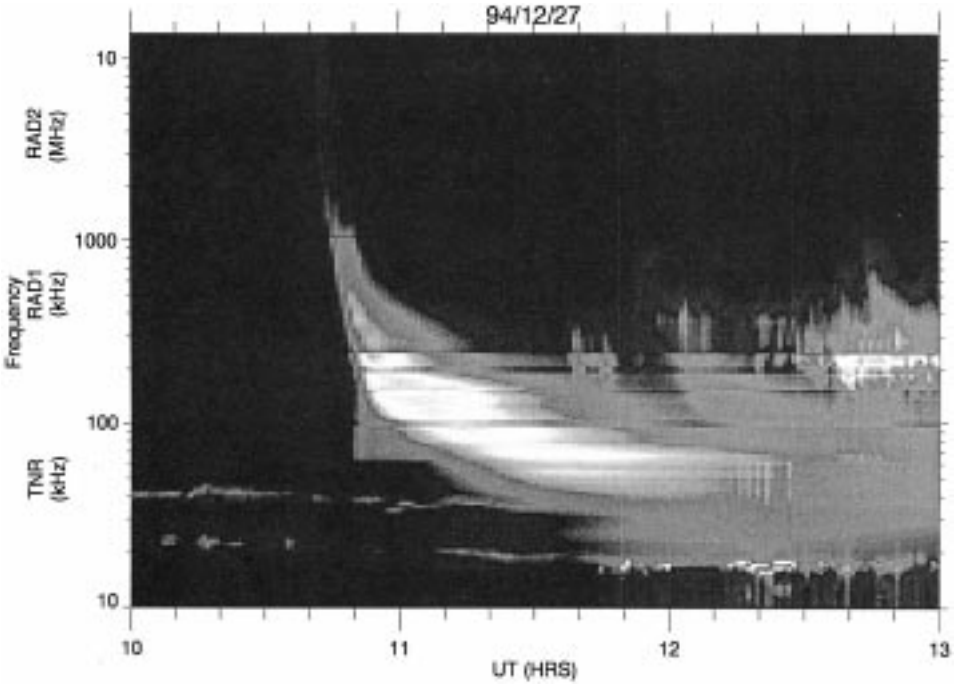

Figure 1. Dynamic spectrum of the type III burst of 1994 December 27, 10:40 UT, as recorded by the radio receivers of *Wind*: RAD2 (13.8–1 MHz), RAD1 (1 MHz–20 kHz), and TNR (250–10 kHz). Auroral kilometric radiation causes the signal concentrated near 300 kHz. The quasi-thermal plasma line is prominent at $f_p \approx 19$ kHz, and its sudden intensification at 1145 UT signals the commencement of Langmuir waves. The 2 f_p line due to electrons from the Earth's bow shock is visible near 40 kHz.

and Δt is the time from burst onset at 13.8 MHz to Langmuir wave onset at 1 AU. The path length along the Archimedean spiral is determined by taking into account the solar wind speed at the time of the type III burst as given in the Key Parameters of ISTP (Ogilvie *et al.*, 1995); in this example, the solar wind speed was 500 km s^{-1} and the spiral path length was 1.10 AU.

Using the derived average speed for this event, 0.13 c, we then add the solid line onto Figure 2, the trace of electrons travelling along the spiral. A correction for light travel has been included in this figure, 500 s for emissions arising at 1 R_0 and proportionally less for those arising between 1 R_0 and 1 AU. We ignore possible time corrections due to scattering of the radiation between the true source and the observer, on the basis that such a correction would be largest for radiation emitted near 0.5 AU, and even there, it should not exceed 2–4 min, which is negligible on the time scale of the relevant frequencies.

The fact that the burst onset times closely track this line up to the onset of the Langmuir waves is conclusive evidence that the radiation is at the fundamental.

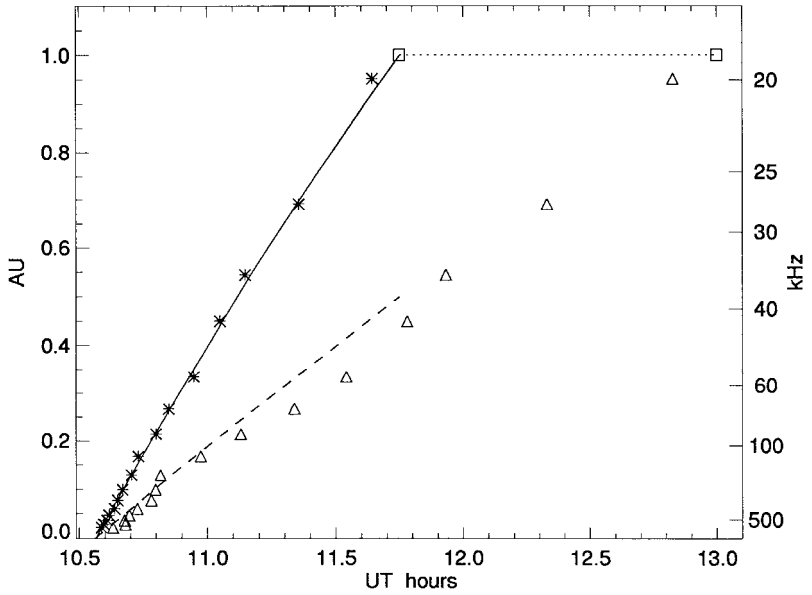

Figure 2. Start times (stars) and times of peak flux density (triangles) of radio waves at different frequencies (right scale) that are emitted at different distances from the Sun (left scale). A correction for light travel time has been included. The squares connected by the dotted line show the interval of Langmuir waves. The solid line is the trace of electrons of $v_{\parallel} = 0.13\ c$ that emit radiation at the fundamental as they travel along an Archimedean spiral from the Sun to *Wind*, starting at the acceleration time as given by the type III burst at high frequencies and arriving at *Wind* at the time of the commencement of Langmuir waves. The dashed line would be the trace of the same electrons if they emitted only harmonic radiation.

If the radiation were at the harmonic, the onset times would track the dashed line which is at twice the frequency of the solid line.

Figure 3(a) shows frequency vs onset time for the frequency range 13.8 MHz to 20 kHz. The measurements in the high-frequency range of the *Wind* receiver, 13.8 to 1 MHz, are shown as diamonds and those below 1 MHz as stars. The square is the local plasma frequency at 1 AU, 19 kHz ($n_e = 4.5\ \mathrm{cm}^{-3}$). The onset time of the burst at 1 R_0, t_{init}, extrapolated from the highest frequencies to 1 R_0 is 10:33:36 UT (vertical asymptote).

The position of the burst source along the Archimedean spiral is calculated for each frequency f_i by the relation: $s_i = v_{\mathrm{elec}}(t_i - t_{\mathrm{init}})$, where t_i is the starting time of the burst at frequency f_i. Then s_i is converted to radial distance r_i. The result is shown in Figure 3(b). For a comparison of our derived densities with an existing model, we add to Figure 3(b) the solid line, the model of Saito *et al.* (1977) normalized to $n_e(1\ \mathrm{AU}) = 4.5\ \mathrm{cm}^{-3}$ (19 kHz). There is good agreement, with the largest differences occurring near 5 R_0.

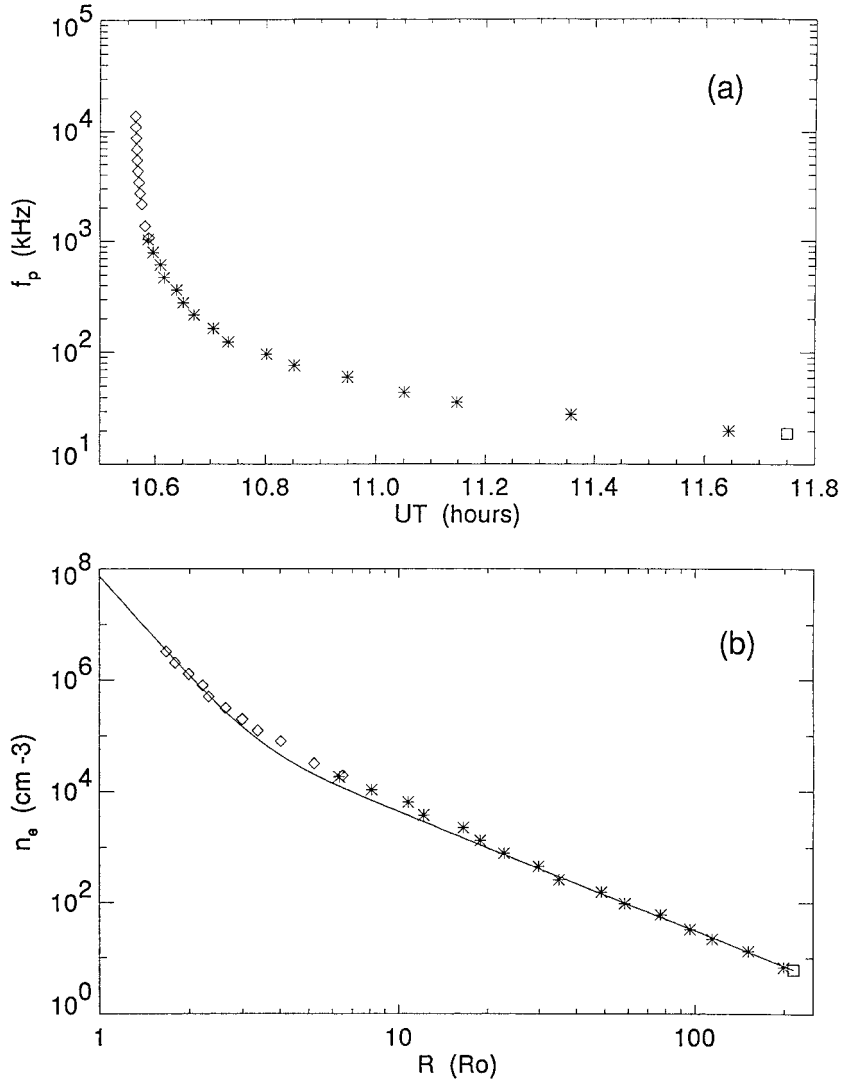

Figure 3. (a). Frequency vs onset time for the type III burst of 27 December 1994. The diamonds and the stars refer respectively to the high- and low-frequency radio receivers of *Wind*. The square denotes the onset time of Langmuir waves at the local plasma frequency at 1 AU. (b). Electron density vs radial distance as derived from the data of the top figure. The position of the burst at each frequency was calculated from knowledge of the average speed of the electrons and the onset times. The solid line shows the Saito *et al.* (1977) model normalized to $n_e = 4.5$ cm^{-3} ($f_p = 19$ kHz) at 1 AU.

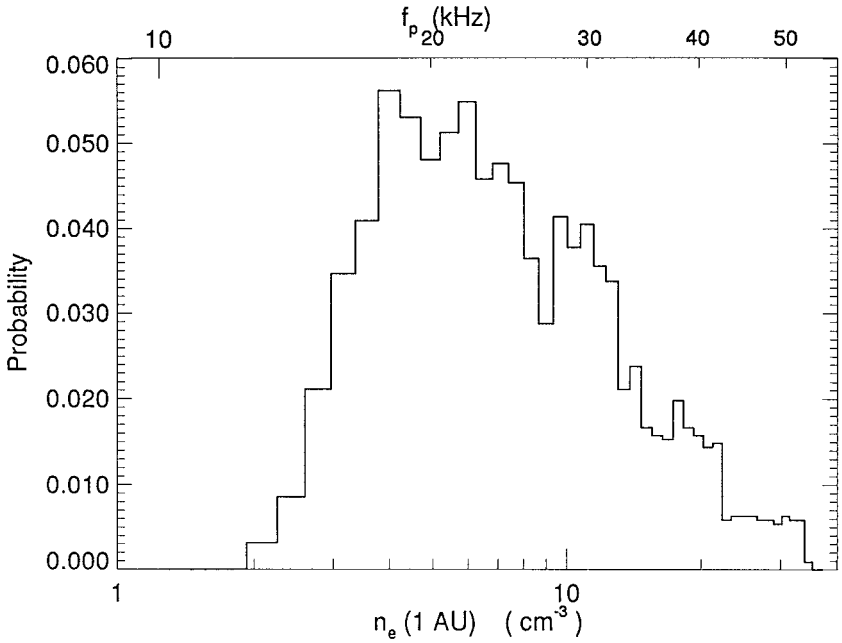

Figure 4. (a). Distribution of electron density at 1 AU at the times of 445 random type III events (fundamental or harmonic) recorded by *Wind*. The median value of n_e is 7.2 cm^{-3}.

3. Electron Density Model

3.1. Density at 1 AU

We proceeded in the same way as above for the other 10 bursts. To derive an average density model we have normalized the plasma frequency at 1 AU to an average value of 24 kHz ($n_e = 7.2$ cm^{-3}). This value pertains to solar activity minimum, as do our data. It is derived from Figure 4 which shows the distribution of electron density at 1 AU (or plasma frequency) at the time of 445 type III bursts observed by *Wind* from 1994 to 1996; the range of f_p at 1 AU is from 13 kHz ($n_e = 3.2$ cm^{-3}) to 55 kHz ($n_e = 39$ cm^{-3}). Therefore the variation in electron density at 1 AU is an order of magnitude. The value $n_e = 7.2$ cm^{-3} is representative of n_e(1 AU) at the times of our observations. It is the same as found by Issautier *et al.* (1997), and very similar to the value of 6.1 of Bougeret, King, and Schwenn (1984).

3.2. Derivation of the model

For our model, we assume that the electron density from the low corona to 1 AU can be described by the relationship

$$n_e = ar^{-2} + br^{-4} + cr^{-6} \, . \tag{1}$$

In this equation the density fall off is steeper close to the Sun than at large distances, which is in agreement with density measurements in the corona.

The term proportional to r^{-2} is dominant from a few tens of R_0 to and beyond 1 AU (hectometric and kilometric frequencies). This dependence is appropriate for the extended solar wind as shown by several authors (Schwenn, 1983; Bougeret, King, and Schwenn, 1984; Issautier *et al.*, 1997). The coefficient a is fixed almost entirely by the density measured by *Wind*, i.e., $n_e(1\ \mathrm{AU})$.

In the corona from ≈ 1.3 to $\approx 3\ R_0$ (decametric frequencies) coronal observations have shown that $n_e \sim r^{-6}$ (Newkirk, 1967; Saito, Poland, and Munro, 1977), which justifies the form of the third term in the equation. To a first approximation, the coefficient c is determined by $n_e(r_o)$, where r_o is the radial distance corresponding to the highest observing frequency f_o (usually 13.8 MHz, in which case $n_e(r_o) = 2.35 \times 10^6\ \mathrm{cm}^{-3}$). The Saito, Poland, and Munro (1977) model, when normalized to $n_e(1\ \mathrm{AU}) = 7.2\ \mathrm{cm}^{-3}$, gives $r_o = 1.83\ R_0$, in which case $c \approx 8.5 \times 10^7$. For other densities at 1 AU, r_o is scaled by $r_o = 1.83(n_e(1\ \mathrm{AU})/7.2)^{1/6}$.

We have added the term proportional to r^{-4} to improve the transition between the corona and the solar wind. The coefficient b is derived from the best least-squares fit of all the data points, and simultaneously the value of c is improved.

Our model does not describe the inner corona below $\approx 1.2\ R_0$ where the density gradient is as high as r^{-16}. For this inner region it is better to use density models derived from eclipse or coronograph observations.

Figure 5 shows all the data points of the derived densities as a function of radial distance. With r in units of R_0, the density model is given by the formula

$$n_e = 3.3 \times 10^5\ r^{-2} + 4.1 \times 10^6\ r^{-4} + 8.0 \times 10^7\ r^{-6}\ \mathrm{cm}^{-3}\ . \tag{2}$$

With R in units of AU (1 AU = 215 R_0) the formula becomes:

$$n_e = 7.2\ R^{-2} + 1.95 \times 10^{-3}\ R^{-4} + 8.1 \times 10^{-7}\ R^{-6}\ \mathrm{cm}^{-3}\ . \tag{3}$$

It can be seen that the solid line representing this equation fits the data points very well particuliarly from 10 to 215 r_o. The dispersion of the data points is largest from about 3 to 20 R_0; the distribution is not gaussian: it is not the result of measurement errors, but of differences in the derived density from one burst to another. Thus it demonstrates that the density distribution along Archimedean spirals does not have a constant form but a changing one. Our model density distribution of Equations (2) and (3) is simply an average over time.

For individual bursts, with different density at 1 AU, the model must be multiplied by a factor derived from the density at 1 AU: $n_e(1\ \mathrm{AU})/7.2$. In doing this, one assumes that there is a steady state from the corona to 1 AU. Often this assumption is valid, at least to a first approximation, and especially near sunspot minimum, as evidenced by steady and slowly varying solar density and speed for hours or days surrounding the type III burst. But it is not always the case, because the base density in active regions may change within the approximately 4 days required for the solar wind to propagate from 1 R_0 to 1 AU. Therefore the density gradient may

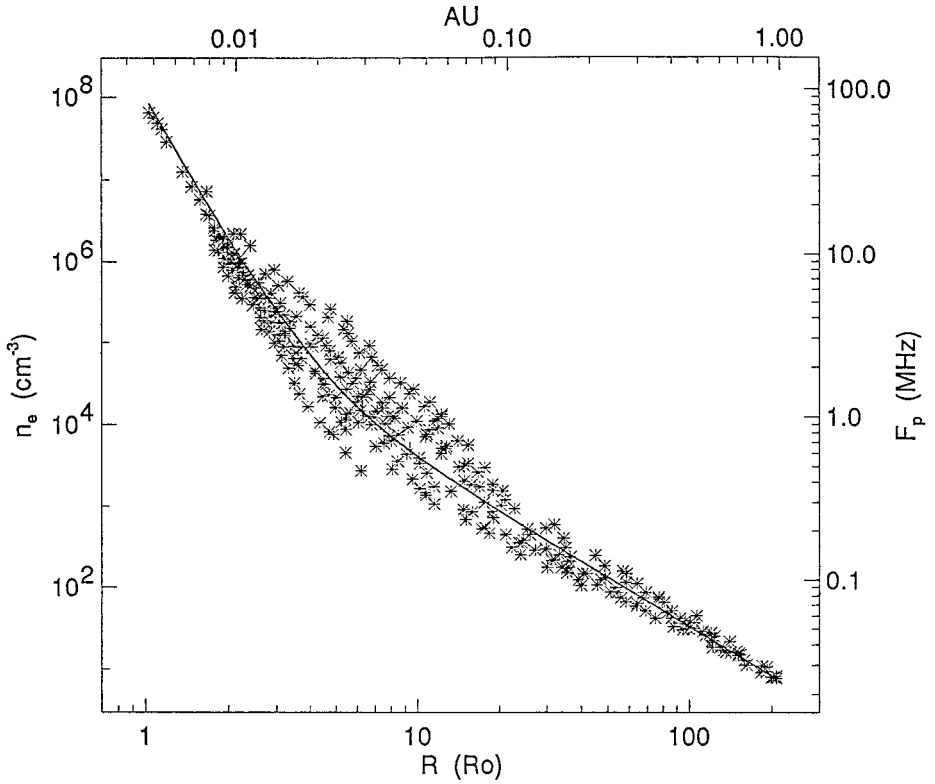

Figure 5. Electron density model vs radial distance derived from all 11 events, where the density at 1 AU has been normalized to 7.2 cm^{-3} ($f_p = 24$ kHz). The solid line is the best fit whose equation is given in the text. The small cluster of points in the upper left comes from 25–75 MHz observations of Nançay for one event.

differ from the steady state at one or more positions along the path of the type III electrons; this is the probable cause of the spread of the data points.

3.3. Comparison with other models

Table I gives the main characteristics of five density models that have been proposed, the equation describing the model, the range of solar radii of the relevant observations, and the density at 1 AU as extrapolated from the equation. These models are representative of *in-situ* measurements (Bougeret, King, and Schwenn, 1984), radio bursts measurements (Alvarez and Haddock, 1973; Fainberg and Stone, 1971), and measurements with a coronograph (Saito, Poland, and Munro, 1977) (see Bougeret, King, and Schwenn (1984) for more details).

Figure 6(a) shows our model (full line) compared with these other models. The lines are thick where the measurements were made: the extrapolations to 1 R_0 and 1 AU were not given by the authors, but were added by us in order to compare

TABLE I
Comparison of density models

Model	Electron density (cm^{-3})	Range (R_0)	n_e(1 AU) (cm^{-3})
LDB[1]	$n_e = 2.8 \times 10^5\, r^{-2} + 3.5 \times 10^6\, r^{-4} + 6.8 \times 10^7\, r^{-6}$	1.8–215	7.2
SPM[2]	$n_e = 1.36 \times 10^6\, r^{-2.14} + 1.68 \times 10^8\, r^{-6.13}$	2.5–5.5	13.9
BKS[3]	$n_e = 4.86 \times 10^5\, r^{-2.10}$	64.0–215	6.1
AH[4]	$n_e = 2.83 \times 10^6\, (r - 0.9)^{-2.15}$	4.8–210	27.6
RAE[5]	$n_e = 5.52 \times 10^7\, r^{-2.63}$	10.0–40	40.5

[1] Leblanc, Dulk, and Bougeret (this paper).
[2] Saito, Poland, and Munro (1977).
[3] Bougeret, King, and Schwenn (1984).
[4] Alvarez and Haddock (1973) (from OGO-5 data only).
[5] Fainberg and Stone (1971).

trends, using the equations in Table I. It is interesting to note that the Saito, Poland, and Munro (1977) model, although derived from measurements in the range of 2 to 5.5 R_0, has a good slope when extrapolated to 1 AU.

For a better comparison, Figure 6(b) shows all these models normalized to $n_e = 7.2$ cm^{-3} at 1 AU. Excepting the RAE model with its very steep density gradient, the agreement is remarkable. In particular the density fall-off being proportional to r^{-2} at $r > 10$ R_0 is in accord with almost all models, and with *in-situ* observations quoted in Section 1.4.

The RAE density model was derived from a type III storm, with the radiation assumed to occur at the fundamental (Fainberg and Stone, 1971). The technique is based on the change of frequency drift rate as the type III storm center moves from disk center toward the limb. It provides the level of separation between different frequencies, which the authors found to be consistent with n_e being proportional to $r^{-2.63}$, where the exponent 2.63 is that of Newkirk's (1967) model; this latter model was derived from observations of the corona at heights less than 5 R_0 where the density gradient is steeper than in interplanetary space. Then the radial distance of the 2.8 MHz plasma level was fixed to be 11.6 R_0, a value that in our model occurs at 3.5 R_0. Later, Fainberg and Stone (1974) recognized that the RAE model implies very high densities that are very rarely observed in interplanetary space, and suggested that the radiation is at the harmonic, thus decreasing the densities by a factor of 4. Bougeret, Fainberg, and Stone (1984) found similar results for other type III storms. However type III storm activity occurs under special conditions that may be not representative of interplanetary space during propagation of isolated type III bursts. In particular, the storm on which the RAE model was based may have occurred in an exceptionally dense region.

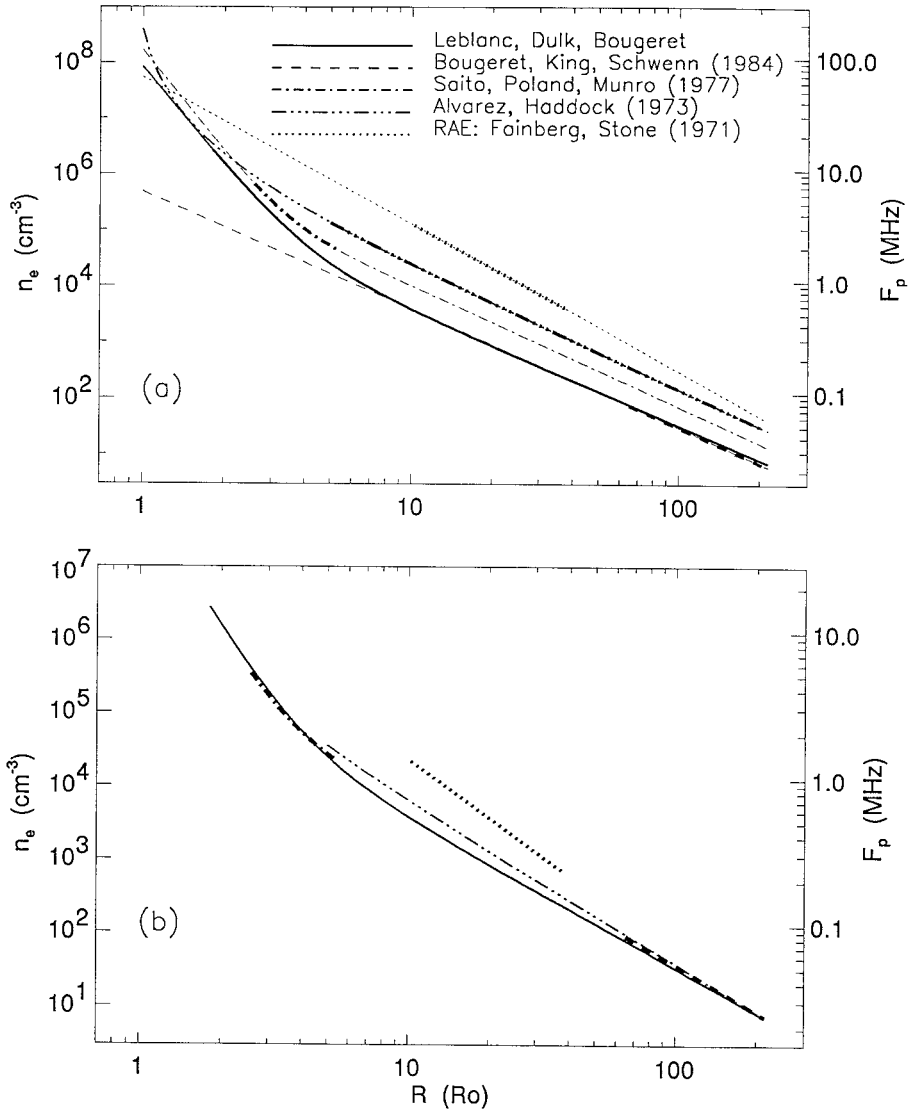

Figure 6. Comparison of different electron density models. In the top figure the lines are thickened in the range of validity given by the authors. In the bottom the same models are shown, normalized to an electron density at 1 AU of 7.2 cm^{-3}.

4. Conclusion

We have derived an electron density model from solar type III bursts observed in the range of 13.8 MHz (1.8 R_0) to $\approx$ 20 kHz (1 AU), extended in one event to 75 MHz (1.3 R_0). This model is not based on an hypothesis of the radiation mode, fundamental or harmonic, because we have used only bursts associated with

Langmuir waves and/or with electron events, which enabled us to find that in all cases the radiation was at the fundamental in the initial part. In addition, the density at 1 AU was derived from the quasi-thermal plasma line, the characteristics of the Archimedean spiral were defined by the measured solar wind speed for each event, and the average speed of the fast electrons was derived from the radio spectra together with times of Langmuir wave or electron events at 1 AU.

The density model derived here from radio observations is in agreement with *in-situ* observations by the *Helios* spacecraft in the range 0.3 to 1 AU, with density models of the corona, and with *Ulysses* measurements of density near the ecliptic plane and density gradient from 1.5 to 2.3 AU at latitudes $\gtrsim 40°$. The agreement is most striking when the models are normalized to a given value of the electron density at 1 AU. There is no need to assume type III electron propagation in overdense structures; neither theory nor observations substantiate that assumption.

The model could be extended down to 1 R_0 by combining ground-based observations in the metric/decametric range and spacecraft observations in the hectometric/kilometric range for the same bursts. However, there are several difficulties: it is essential to accurately measure the start times of a given burst over the entire frequency range. But in the high-frequency range, type IIIs often appear as complex groups of bursts, and usually these groups merge to give rise to one isolated burst at lower frequencies (e.g., Figure 3 of Dulk *et al.*, 1997). In these groups the most intense ones are not necessarily the ones that continue to low frequencies; instead weak ones may become stronger with decreasing frequency and strong ones may become weaker. Therefore the continuity of a given burst from high to low frequencies is often ambiguous. In addition, accurate time resolutions are required, a fraction of a second at the higher frequencies, often exceeding the capabilities of ground-based and space-based instruments. At this time it is better to use coronal models derived from eclipse or coronoraph observations for the low corona.

With the WAVES instrument a few type II bursts have been observed in this large frequency range (Reiner, Kaiser, and Bougeret, 1998). The knowledge of the shock wave velocity is dependent on the electron density model. This parameter is very important for many studies. Thus it is necessary to use a realistic model taking into account the density at 1 AU.

Acknowledgements

The WAVES experiment on *Wind* spacecraft is a joint project of the Observatoire de Paris, NASA/GSFC and the University of Minnesota. The solar wind speeds were measured by the SWE team (Ogilvie *et al.*, 1995) and reported in the Key Parameter list of the ISTP. We thank R. P. Lin for information on solar electron events, P. Zarka and L. Denis for help in obtaining the Nançay decameter spectrum for one event, C. Perche for preparing Figure 1, and S. Hoang, M. Poquerusse and J. L. Steinberg for helpful comments.

References

Alvarez, H. and Haddock, F. T.: 1973, *Solar Phys.* **29**, 197.
Baumbach, S.: 1937, *Astron. Nachr.* **263**, 121.
Boischot, A. *et al.*: 1980, *Icarus* **43**, 399.
Bougeret, J.-L., Fainberg, J., and Stone, R. G.: 1984, *Astron. Astrophys.* **141**, 17.
Bougeret, J.-L., King, J. H., and Schwenn, R.: 1984, *Solar Phys.* **90**, 401.
Bougeret, J.-L. *et al.*: 1995, *Space Sci. Rev.* **71**, 231.
Davis, W. D. and Feynman, J.: 1977, *J. Geophys. Res.* **82**, 4699.
Dulk, G. A., Steinberg, J. L., and Hoang, S.: 1984, *Astron. Astrophys.* **141**, 30.
Dulk, G. A., Steinberg, J. L., Hoang, S., and Goldman, M. V.: 1987, *Astron. Astrophys.* **173**, 366.
Dulk, G. A., Leblanc, Y., Robinson, P. A., Bougeret, J. L., and Lin, R. P.: 1998, *J. Geophys. Res.* **103**, 17223.
Fainberg J. and Stone, R. G.: 1971, *Solar Phys.* **17**, 392.
Fainberg J. and Stone, R. G.: 1974, *Space Sci. Rev.* **16**, 145.
Gurnett, D. A., Baumback, M. M., and Rosenbauer, H.: 1978, *J. Geophys. Res.* **83**, 616.
Haddock, F. T. and Alvarez H.: 1973, *Solar Phys.* **29**, 183.
Hartz, T. R.: 1969, *Planet. Space Sci.* **17**, 267.
Hoang, S., Dulk, G. A., and Leblanc, Y.: 1994, *Astron. Astrophys.* **289**, 957.
Issautier, K., Meyer-Vernet, N., Moncuquet, M., and Hoang, S.: 1997, *Solar Phys.* **172**, 335.
Issautier, K., Meyer-Vernet, N., Moncuquet, M., and Hoang, S.: 1998, *J. Geophys. Res.* **103**, 169.
Kellogg, P.: 1980, *Astrophys. J.* **236**, 696.
Koutchmy S. and Livshits, M.: 1992, *Space Sci. Rev.* **61**, 393.
Kundu, M. R., Gergely, T. E., Turner, P. J., and Howard, R. A.: 1983, *Astrophys. J.* **269**, L67.
Leblanc, Y.: 1973, *Astrophys. Lett.* **14**, 41.
Leblanc, Y. and de la Noe, J.: 1977, *Solar Phys.* **52**, 133.
Leblanc, Y., Leroy, J. L., and Pecantet, P.: 1973, *Solar Phys.* **31**, 343.
Leblanc, Y., Kuiper, T. B. H., and Hansen, S. F.: 1974, *Solar Phys.* **37**, 215.
Lin, R. P. *et al.*: 1995, *Geophys. Res. Lett.* **23**, 1211.
Malitson, H. H., Fainberg, J., and Stone, R. G.: 1973, *Astrophys. J.* **183**, L35.
Melrose, D. B.: 1982, *Solar Phys.* **79**, 173.
Meyer-Vernet, N. and Perche, C.: 1989, *J. Geophys. Res.* **94**, 2405.
Newkirk, G. A.: 1967, *Ann. Rev. Astron. Astrophys.* **5**, 213.
Ogilvie, K. W. and 17 others: 1995, *Space Sci. Rev.*, **71**, 55.
Poquerusse, M., Hoang, S., and Bougeret, J.-L.: 1996, in D. Winterholter *et al.* (eds.), *Solar Wind 8 Conference Proceedings*, AIP Press, Woodbury, New York, p. 62.
Poquerusse, M., Steinberg, J.-L., Caroubalos, C., Dulk, G. A., and MacQueen, R. M.: 1988, *Astron. Astrophys.* **192**, 323.
Reiner, M. J., Kaiser, M. L., and Bougeret, J.-L.: 1998, *Proc 31st ESLAB Symposium, Correlated Phenomena at the Sun, in the Heliosphere, and in Geospace* European Space Agency, Noordwijk, Netherlands, p. 183.
Reiner, M. J., Kaiser, M. L., Fainberg, J., and Stone R. G.: 1998, *J. Geophys. Res.*, in press.
Robinson, P. A.: 1996, *Solar Phys.* **168**, 357.
Saito, K.: 1970, *Ann. Tokyo Astron. Obs. Ser.* **2**, 12, 53.
Saito, K., Poland, A. J., and Munro, R. H.: 1977, *Solar Phys.* **55**, 121.
Schwenn, R,: 1983, in M. Neugebauer (ed), *Solar Wind Five*, NASA CP-2280, p. 489.
Steinberg, J. L., Aubier, M. G., Leblanc, Y., and Boischot, A.: 1971, *Astron. Astrophys.* **10**, 362.
Steinberg J. L., Dulk, G. A., Hoang, S., Lecacheux, A., and Aubier, M.: 1984, *Astron. Astrophys.* **140**, 39.
Stewart, R. T.: 1976, *Solar Phys.* **50**, 437.

Stone, R. G: 1980, in M. R. Kundu and T. E. Gergely (eds), 'Radiophysics of the Sun', *IAU Symp*. **86**, 405.
Van de Hulst, H. C.: 1950, *Bull. Astron. Inst. Neth.* **11**, 135.
Vibert, V.:1997, Thèse de Doctorat de l'Université de Paris.
Wild, J. P., Sheridan, K. V., and Neylan, A. A.: 1959, *Austr. J. Phys.* **12**, 369.
Wild, J. P., Smerd, S. F., and Weiss, A. A.: 1963, *Ann. Rev. Astron. Astrophys.* **1**, 291.